Available online at www.sciencedirect.com

ScienceDirect

Ceramics International 41 (2015) 1823–1829

CERAMICS INTERNATIONAL

www.elsevier.com/locate/ceramint

Effect of ZrB_2 and SiC distributions on the ablation of modified carbon/carbon composites

Lei Liu, Hejun Li*, Yudan Zhang, Xiaohong Shi, Qiangang Fu, Wei Feng, Tao Feng

State Key Laboratory of Solidification Processing, Northwestern Polytechnical University, Xi'an 710072, Shaanxi, PR China

Received 9 July 2014; received in revised form 23 September 2014; accepted 26 September 2014
Available online 6 October 2014

Abstract

To understand the effect of introduced phases' distribution on the ablation of carbon/carbon (C/C) composites, C/C–ZrB_2–SiC composites containing isolated (SZ-1) and coupled (SZ-2) ZrB_2–SiC particles were prepared via controllable precursor infiltrations and pyrolysis, respectively. Ablation under oxyacetylene torch at both *Z* and *XY* directions showed that SZ-1 had better ablation resistance than SZ-2, while the surface temperature rose up to about 2400 °C. The ablated surface morphologies showed that a relative integrate layer of ablation products was formed on SZ-1, whereas the layer on SZ-2 was defective. It was believed that the dissimilar distributions of ZrB_2–SiC particles in composites resulted in distinct structures of ablation products on the surfaces and consequently their different ablation behavior.

Keywords: B. Composites; C. Corrosion; D. Carbon; D. SiC; Distribution

1. Introduction

As one of the most promising materials for aerospace application, carbon/carbon (C/C) composites were extensively investigated aiming at the challenge to improve their oxidation [1–3] and ablation [4–6] resistances. Most of these works focused on modification of C/C composites by SiC and ultra high temperature ceramics (UHTC). A well-designed coating always offered a reliable ablation resistance for a short-term ablation [7–9], while introduction of SiC and UHTC into C/C composites was necessary for the practical application in long-term service [10]. Content of introduced phases was firstly studied for modified C/C composites and results preferred a higher ceramic volume [11,12]. Furthermore, other factors such as the architecture of the carbon fabric [13], the original density of C/C composites' preform [14] and the thickness of the interface, [15] were proved to be important to the fabrication and ablation of the modified C/C composites. Employing UHTC in various types was also studied [16–18]. Nevertheless, balancing an optimal ratio of these UHTCs was a challenging and enduring topic in the last several years, since the application environment of components in aerospace vehicles is always various and complicated [19–21]. However, how does the distribution of introduced phases affect the ablation of modified C/C composites was rarely reported. In order to take a better advantage of the UHTCs in C/C composites for improving the ablation resistance, it is necessary to make a further investigation to figure out the effect of introduced phases' distribution on the ablation resistance.

In the present work, C/C–ZrB_2–SiC composites containing isolated (SZ-1) and coupled (SZ-2) ZrB_2–SiC particles were prepared by controlling the process of precursor infiltrations and pyrolysis (PIP). Ablation tests at *Z* and *XY* directions under oxyacetylene torch were performed to investigate the distribution's effect on the ablation resistance. Ablated surface morphologies provided a good hint to clarify the different ablation behavior.

*Corresponding author. Tel.: +86 29 88495004; fax: +86 29 88492642.
E-mail address: lihejun@nwpu.edu.cn (H. Li).

http://dx.doi.org/10.1016/j.ceramint.2014.09.129
0272-8842/

2. Experimental procedure

2.1. Composites preparation

The layers of 0° non-woven fiber cloth, chopped fiber web and 90° non-woven fiber cloth were overlapped on each other subsequently, with needle-punching step by step, T300 PAN-based carbon fibers were fabricated as reinforcement (0.45 g/cm^3). The reinforcement was densified to 0.63 g/cm^3 (as shown in Fig. 1 (a)) by thermal gradient chemical vapor infiltration (TCVI) at 950–1150 °C. Methane was used as carbon source. And then ceramic particles were introduced into the preform by traditional PIP. Two types of distributions for both ZrB_2 and SiC in the preform, isolated and coupled, were obtained via the different PIP process (as shown in Fig. 1(b)). In brief, we employed dimethylbenzene as solvent to dissolve a certain amount of polycarbosilane (PCS, ceramic production ration was about 64 wt%) denoted as Solution A and ZrB_2 precursor (purchased from Chinese Academy of Sciences, ceramic production ratio was about 33 wt%) as Solution B by ultrasonic method for 1 h, respectively. After immersing the perform in the as-prepared Solution A under vacuum, the sample was dried at 70–90 °C and then were subjected to a heat treatment at 1500–1800 °C for 2 h in a flowing Ar atmosphere, SiC was firstly infiltrated and deposited into the preform. Afterwards in Solution B, ZrB_2 was then introduced into the preform similarly. As a result, the isolated ZrB_2–SiC in SZ-1 were prepared. The PIP in preparing SZ-2 was the same as described above except for a single mixed solution of ZrB_2 precursor and PCS instead of the two solutions. The mass of ceramic particles in a composite was calculated according to Eq. (1).

$$m_{\text{ceramic}} = m_1 - m_0 \tag{1}$$

where m_0 and m_1 are the mass of a preform before impregnation and after heat treatment.

The increasing of composites' densities with cycles of PIP is shown in Fig. 1(c). Once the ceramic contents in the two composites reached the target level, the doped preforms were finally densified through TCVI. The content of ZrB_2–SiC particles in the fabricated composites was about 20 wt% while the mass ratio of ZB_2 and SiC was 3:2. The densities of these two composites were 1.83 g/cm^3 (SZ-1) and 1.82 g/cm^3 (SZ-2), respectively.

As shown in Fig. 1(d), bar-like samples (55 × 10 × 4 mm) were cut from the prepared composites for three-point bending test, disk (Φ30 × 10 mm) and cubic (10 × 10 × 10 mm) samples were cut and lightly abraded with 80 and 400 grit SiC paper for ablation test.

2.2. Tests and characterization

Three-point bending test was performed on the electronic universal testing machine (CMT 5304, Suns Co. China). The support span was 40 mm, and the ratio of span-to-thickness was 10:1. The ultimate value was averaged from five samples tested with a crosshead speed of 0.5 mm/min.

The ablation test was carried out in oxyacetylene torch with heat fluxes of 2.38 MW/m^2. The pressure of O_2 and C_2H_2 were 0.4 and 0.095 MPa and their fluxes were 0.24 and 0.18 L/s, respectively. The inner diameter of the oxyacetylene gun tip was 2 mm, and the distance between the gun tip and the sample was 10 mm. The ablation angle was kept at 90°, and the ablation was performed at *Z* (disk samples) and *XY* (cubic samples) directions, respectively. The linear and mass ablation rates were calculated according to Eqs. (2) and (3). The ultimate data was averaged from three samples.

$$R_l = \frac{\Delta d}{t} \tag{2}$$

$$R_m = \frac{\Delta m}{t \times A} \tag{3}$$

R_l is linear ablation rates; Δd is the change of the sample's thickness at centre region before and after ablation; R_m is mass ablation rates; Δm is the change of the mass before and after

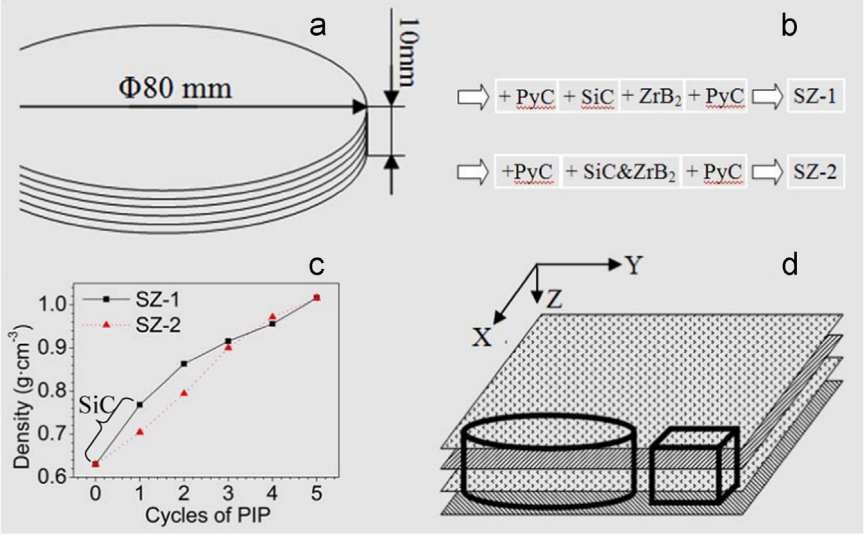

Fig. 1. The flowchart of the process for preparing two different C/C–ZrB_2–SiC composites: (a) discal preform used for fabricating composites; (b) procedure of preparing SZ-1 and SZ-2; (c) increasing of composites' densities with cycles of PIP; (d) obtaining of samples for ablation and three point bending test.

ablation; t is ablation time which is controlled at 180 s, A is area of front face of sample.

The surface temperature was measured by an infrared thermometer (Raytek MR1SCSF) in 2-color mode with the error of $\pm 0.75\%$. The phase analysis of composites before and after ablation was conducted by X-ray diffraction (XRD, X'Pert Pro MPD). Morphologies and chemical compositions of the prepared and ablated composites were investigated by scanning electron microscope (SEM, JSM6460) equipped with energy dispersive spectroscopy (EDS).

3. Results and discussion

3.1. Microstructure

Fig. 2 shows the cross-sectional morphologies of the prepared composites and relative EDS analysis. At the lower magnification, no obvious difference between SZ-1 and SZ-2 was observed. Both composites are composed of black phase, white particles and some pores (Fig. 2(a)). These doped ceramics are in the forms of discontinuous particles which are distributed uniformly in the composites. Moreover, three-point bending test shows that the two composites have similar bending strength (98 ± 11 MPa) and modulus (14 ± 1.5 GPa). However, the disparity in morphology between them is discernable at higher magnification of SEM images (Fig. 2(b)–(e)). Combined with XRD patterns (Fig. 4(g)), EDS analysis proves that the black phase is carbon, the white particles are ZrB_2 and the grey phase is SiC. For SZ-1 (Fig. 2(b) and (d)), ZrB_2 and SiC are isolated and ZrB_2 particles are placed between SiC and carbon. However, the ZrB_2 and SiC particles in SZ-2 (Fig. 2(c) and (e)) are coupled together in a smaller size where most of these ZrB_2 particles are enwrapped by SiC. As well known, SiC is consumed faster than pyrocarbon and loses its protective effect at high temperature over 2000 °C [22]. Therefore, it is supposed that the ablation behavior of these two composites will be differed by the two distributions of ZrB_2–SiC.

Fig. 3 displays the ablation rates of SZ-1 and SZ-2 at two directions. It shows SZ-1 has lower linear and mass ablation rates than SZ-2 at both Z and XY directions, which means, SZ-1 has better ablation property. In addition, ablation at XY direction is worsened than that at Z direction for both composites. This is similar to the ablation of C/C composites [23].

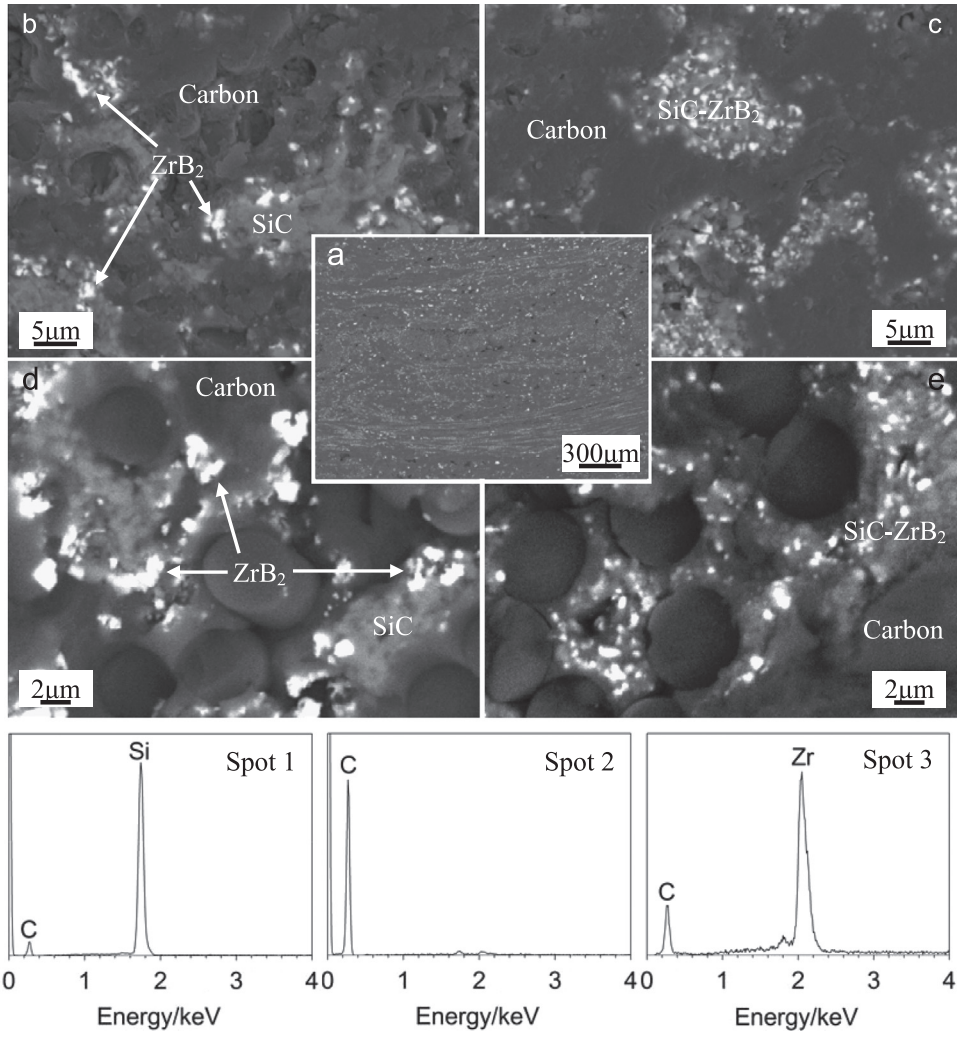

Fig. 2. Cross-sectional morphologies of prepared composites and relative EDS analysis: (a) low magnification of SZ-1; ((b) and (d)) SZ-1; ((c) and (e)) SZ-2.

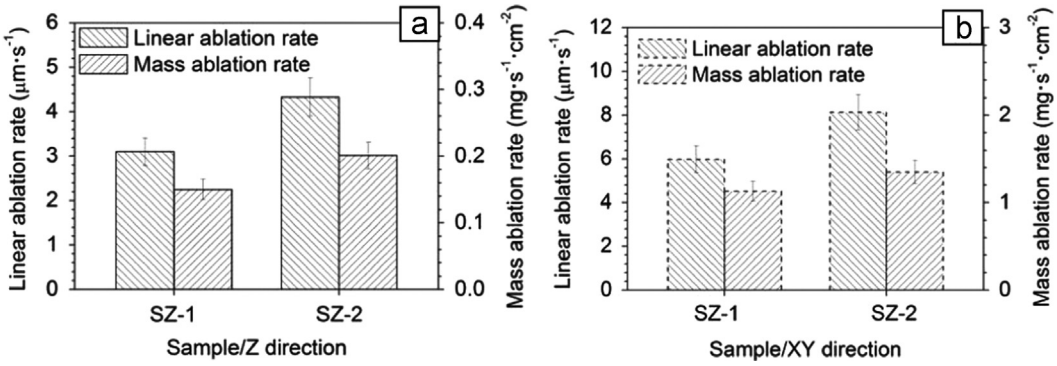

Fig. 3. Ablation rates of prepared composites at different directions: (a) *Z* direction; (b) *XY* direction.

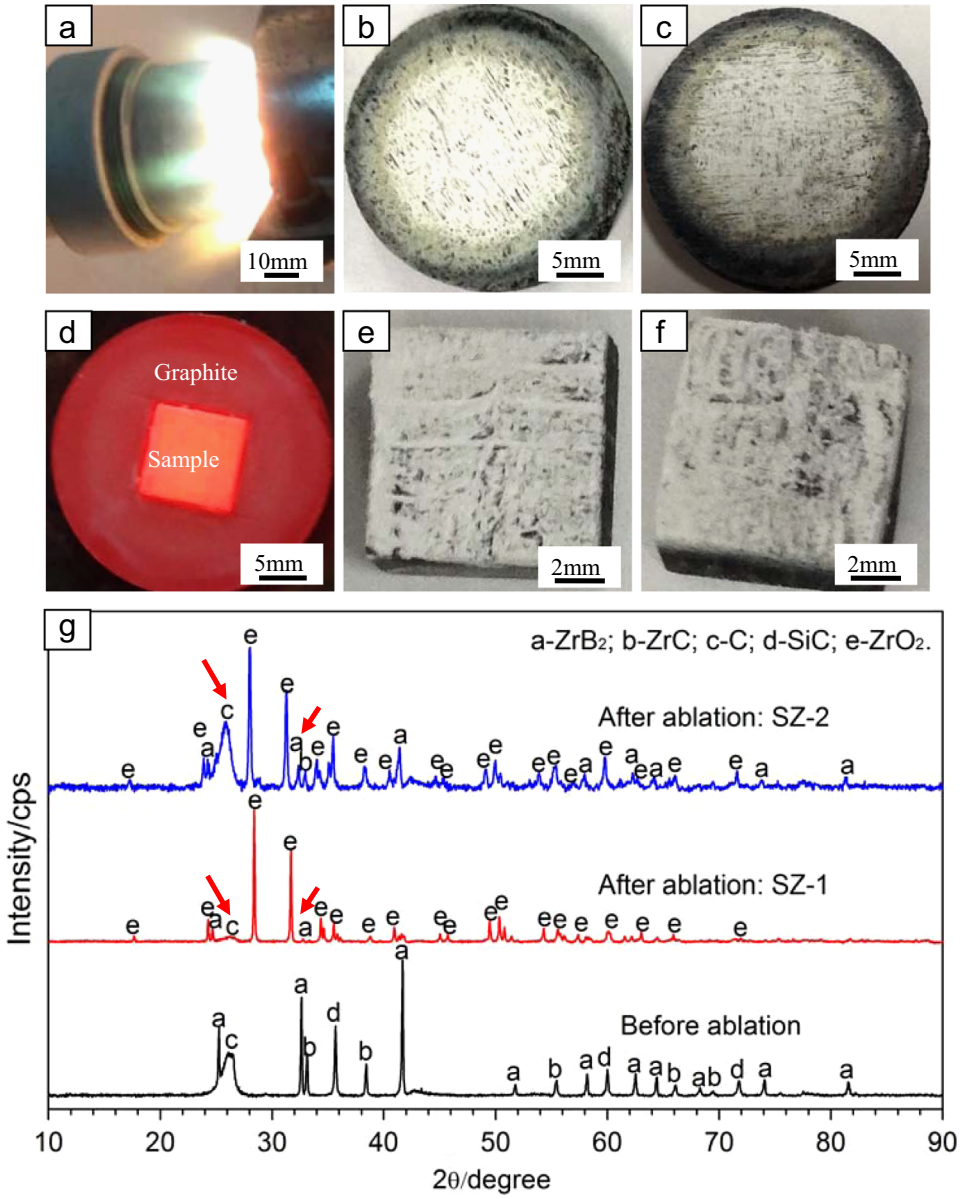

Fig. 4. Photography of the flame during ablation, ablated samples and relative XRD patterns: (a) flame during ablation; (b) SZ-1 at *Z* direction; (c) SZ-2 at *Z* direction; (d) *XY* directional sample and its clamp; (e) SZ-1 at *XY* direction; (f) SZ-2 at *XY* direction; (g) XRD patterns of prepared composites before and after ablation. (For interpretation of the references to color in this figure legend, the reader is referred to the web version of this article.)

The photography of the flame during ablation, ablated samples and relative XRD patterns are shown in Fig. 4. Obviously, the color of peripheral flame is light green due to the combustion of Boron-containing products (Fig. 4(a)). To perform the ablation at *XY* direction, cubic samples was fixed by a graphite clamp (Fig. 4(d)). From the macro-morphologies of the ablated samples in Fig. 4(b), (c), (e) and (f), it can be found that a lot of white phases covers on the front surface of sample and forms a layer of ablation products. This phenomenon was also reported in other works [24,25]. Some defects could be observed on this white layer of SZ-2 while that layer of SZ-1 is relatively integrated. XRD patterns prove that the layer of ablation products on both composites is mainly composed of ZrO_2. However, in SZ-2, the XRD intensities of graphite carbon and ZrB_2 phases compared to ZrO_2 phase are stronger than those in SZ-1 (indicated by arrows in Fig. 4(g)). By combining the XRD analysis and macro-morphologies comparison after ablation, it can be inferred that the layer of ablation products on SZ-1 is more integrate or thicker than that of SZ-2.

Fig. 5 shows the recorded central surface temperature and the SEM morphologies of two prepared composites after ablation for further comparison. As a result of being heated by oxyacetylene torch meanwhile with the formation and accumulation of ablation products, the central surface temperature rises to about 2400 °C for all tested samples. Under such an oxygen-rich environment, composites will be oxidized and SiO_2 is not able to endure such high temperature due to the high vapor pressure. Thus, absence of SiO_2 (Fig. 4(g)) on the ablated outer surface is reasonable. Besides, the fast cooling process from 2400 °C to below 1000 °C within several seconds after ablation prefers the formation of amorphous SiO_2 residuals which results in undetectable SiO_2 crystalline peaks in XRD. By comparing the morphologies after ablation (Fig. 5(b)–(e)), it can be found that the layer of ablation products on the outer surface of SZ-2 has more visible defects (region M and N) than that of SZ-1. This is consistent with the macro-morphologies shown in Fig. 4. To further study the ablation of these two composites, region A/E, B/F, C/G and D/H were marked on the surface for the following analysis.

Fig. 6 shows the morphologies of outer surface and sub-layer of the ablation products. Corresponding to the marked regions in Fig. 5, details of ZrO_2 layer on the surface can be revealed. Continuous ZrO_2 layer contains some cracks on the surface of SZ-1, while plenty of pores are in ZrO_2 layer of SZ-2. Besides, the partially sintered ZrO_2 particles (Fig. 6(a) inset) in SZ-1 are larger than those in SZ-2 (Fig. 6(b) inset), which accords to the sizes of ZrB_2 before ablation. Therefore, by comparing the morphologies at both macro and micro scales, it can be concluded that SZ-2 definitely has more defects situated in the layer of ablation products which is undesired for ablation protection than SZ-1.

After ablation, the surface temperature of the sample drops from 2400 °C to room temperature. This leads to phase transition of the ZrO_2 layer with volume changes. Then the layer of ablation products is easy to be peeled off. Cleaned by aurilave, the sub-layers of ablation products of these two composites are shown in Fig. 6(c)–(f). Although the morphologies are various, one difference between the two composites can be concluded easily: the outer layer of ZrO_2 in SZ-1 covers on substrate of carbon and SiO_2 whereas the ZrO_2 layer of SZ-2 is supported by SiO_2. As mentioned above, the ablation lasts for

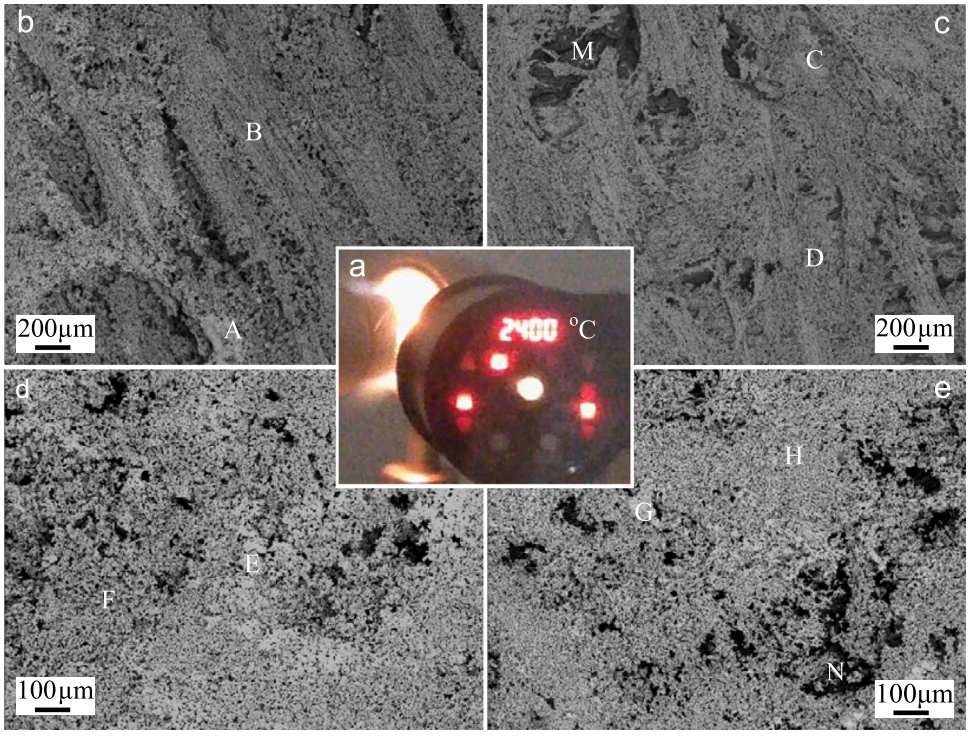

Fig. 5. Central surface morphologies of ablated samples: (a) recorded central surface temperature during ablation; (b) SZ-1 at *Z* direction; (c) SZ-2 at *Z* direction; (d) SZ-1 at *XY* direction; (e) SZ-2 at *XY* direction.

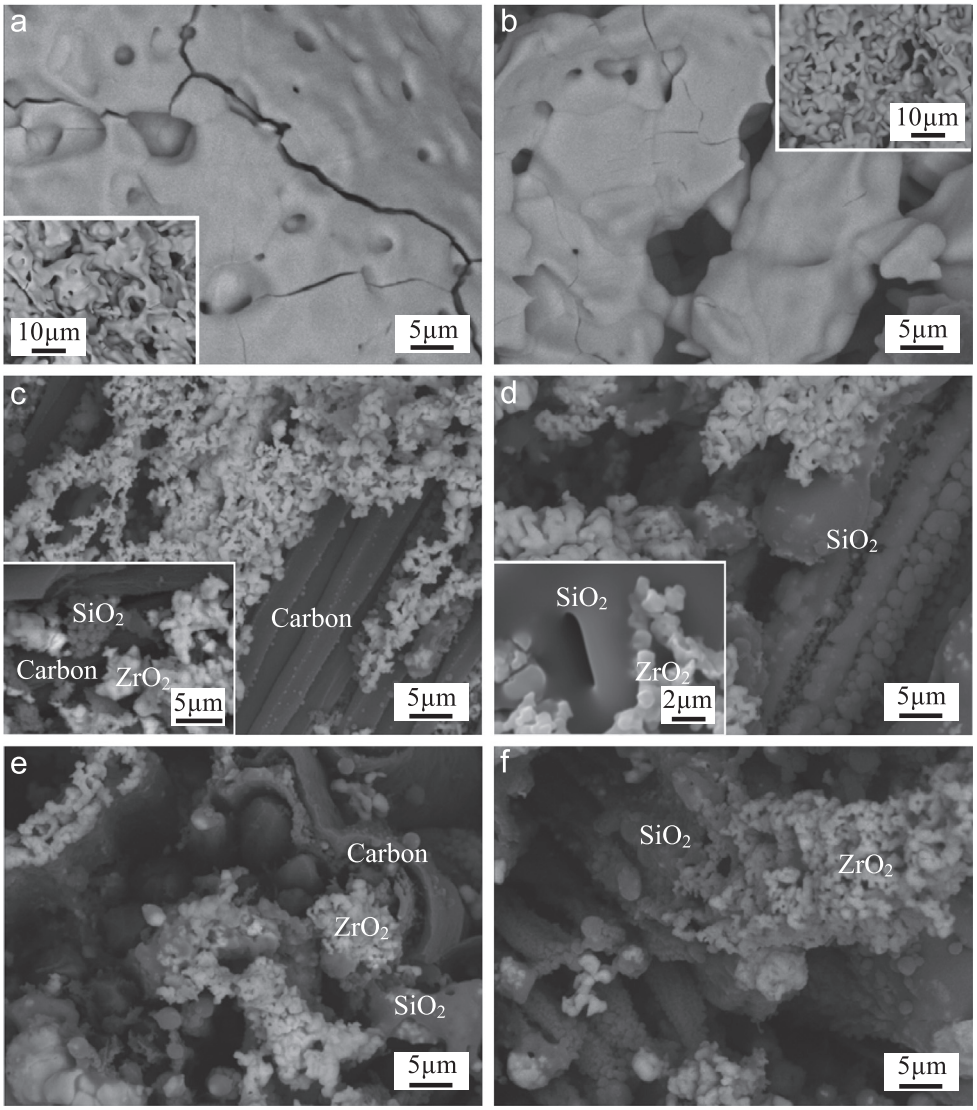

Fig. 6. Magnification of marked regions in Fig. 5 and sub-layer of ablation products: (a) region A/E; (b) region C/G; inset of (a): region B/F; inset of (b) region D/H; (c) sub-layer of SZ-1 at *Z* direction; (d) sub-layer of SZ-2 at *Z* direction; inset of (c): distribution of residual phases at sub-layer of SZ-1; inset of (d): distribution of residual phases at sub-layer of SZ-2; (e) sub-layer of SZ-1 at *XY* direction; (f) sub-layer of SZ-2 at *XY* direction.

180 s and the surface temperature rises to 2400 °C, all of the following reactions possibly proceeded in tested composites:

$$2C(s)+O_2(g)\rightarrow 2CO(g) \quad (4)$$

$$2SiC(s)+3O_2(g)\rightarrow 2SiO_2(l)+2CO(g) \quad (5)$$

$$2ZrB_2(s)+5O_2(g)\rightarrow 2ZrO_2(s)+2B_2O_3(g) \quad (6)$$

$$2ZrC(s)+3O_2(g)\rightarrow 2ZrO_2(s)+2CO(g) \quad (7)$$

$$SiO_2(l)+C(s)\rightarrow SiO(g)+CO(g) \quad (8)$$

$$SiO_2(l)+CO(g)\rightarrow SiO(g)+2CO_2(g) \quad (9)$$

$$SiO_2(l)\rightarrow SiO_2(g) \quad (10)$$

SiC would be consumed faster than pyrocarbon through Eqs. (8)–(10). Besides, ablation of SiC would be accelerated by nearby ZrO_2 since the thermal conductivity of ZrO_2 is very low and SiC could not endure high heat in comparison with pyrocarbon [26]. During the reaction and evaporation of SiO_2, many ZrB_2/ZrO_2 particles in SZ-2 would be scoured away by the oxyacetylene torch before sintered since they are enwrapped by or adhering to SiC/SiO_2. Then some defects in the layer of ablation products of SZ-2 come into being. On the contrast, for the ZrB_2/ZrO_2 in SZ-1 covering above carbon and SiC/SiO_2, the relative steady substrate could prevent more ZrB_2/ZrO_2 from being peeled off. As a result, the more integrated white layer of ablation products on SZ-1 benefits to resist the ablation while fewer ZrO_2 surviving from flame scouring in SZ-2 causes the higher ablation rates.

4. Conclusion

Isolated and coupled ZrB_2–SiC particles were introduced into C/C composites through different PIP methods. Ablation

under oxyacetylene torch at both *Z* and *XY* directions showed that SZ-1 had better ablation resistance than SZ-2 while the surface temperature rose up to about 2400 °C. Ablated central surface morphologies displayed that a relative integrate layer of ablation products was formed on the surface of SZ-1 whereas the layer on SZ-2 was defective. The dissimilar distributions of ZrB_2–SiC particles in composites led to distinct structures of ablation products on the surface, which dominated their ablation behavior.

Acknowledgements

This work has been supported by the National Natural Science Foundation of China under Grant nos. 51202193 and 51221001, the Fundamental Research Foundation of Northwestern Polytechnical University under Grant no. GBKY1021, the Research Fund of State Key Laboratory of Solidification Processing (NWPU), China (Grant no. 25-TZ-2009) and the "111" Project under Grant no. B08040.

References

[1] Y.H. Chu, H.J. Li, Q.G. Fu, H.P. Wang, X.H. Hou, X. Zou, et al., Oxidation protection of C/C composites with a multilayer coating of SiC and Si+SiC+SiC nanowires, Carbon 50 (2012) 1280–1288.

[2] X.R. Ren, H.J. Li, Q.G. Fu, Y.H. Chu, K.Z. Li, TaB_2–SiC–Si multiphase oxidation protective coating for SiC-coated carbon/carbon composites, J. Eur. Ceram. Soc. 33 (2013) 2953–2959.

[3] X.F. Lu, P. Xiao, Short time oxidation behavior and residual mechanical properties of C/C composites modified by in situ grown carbon nano fibers, Ceram. Int. 40 (2014) 10705–10709.

[4] D.D. Jayaseelan, R.G. Sa, P. Brown, W.E. Lee, Reactive infiltration processing (RIP) of ultra high temperature ceramics (UHTC) into porous C/C composites tubes, J. Eur. Ceram. Soc. 31 (2011) 361–368.

[5] Y. Zeng, X. Xiong, G.D. Li, Z.K. Chen, W. Sun, D.N. Wang, Microstructure and ablation behavior of carbon/carbon composites infiltrated with Zr–Ti, Carbon 54 (2013) 300–309.

[6] Y.Y. Cui, A.J. Li, B. Li, X. Ma, R.C. Bai, W.G. Zhang, et al., Microstructure and ablation mechanism of C/C–SiC composites, J. Eur. Ceram. Soc. 34 (2014) 171–177.

[7] Y.L. Wang, X. Xiong, G.D. Li, H.F. Liu, Z.K. Chen, W. Sun, Ablation behavior of HfC protective coatings for carbon/carbon composites in oxyacetylene combustion flame, Corros. Sci. 65 (2012) 549–555.

[8] T. Feng, H.J. Li, X.H. Shi, X. Yang, S.L. Wang, Oxidation and ablation resistance of ZrB_2–SiC–Si/B-modified SiC coating for carbon/carbon composites, Corros. Sci. 67 (2013) 292–297.

[9] S.L. Wang, K.Z. Li, H.J. Li, Y.L. Zhang, Microstructure and ablation resistance of ZrC nanostructured coating for carbon/carbon composites, Mater. Lett. 107 (2013) 99–102.

[10] C.Y. Li, K.Z. Li, H.J. Li, H.B. Ouyang, Y.L. Zhang, L.J. Guo, Ablation resistance and thermal conductivity of carbon/carbon composites containing hafnium carbide, Corros. Sci. 75 (2013) 169–175.

[11] X.T. Shen, K.Z. Li, H.J. Li, Q.G. Fu, S.P. Li, F. Deng, The effect of zirconium carbide on ablation of carbon/carbon composites under an oxyacetylene flame, Corros. Sci. 53 (2011) 105–112.

[12] H.J. Li, D.J. Yao, Q.G. Fu, L. Liu, Y.L. Zhang, X.Y. Yao, Anti-oxidation and ablation properties of carbon/carbon composites infiltrated by hafnium boride, Carbon 52 (2013) 418–426.

[13] Y. Zeng, X. Xiong, G.D. Li, Z.K. Chen, W. Sun, D.N. Wang, et al., Effect of fibre architecture and density on the ablation behavior of carbon/carbon composites modified by Zr–Ti–C, Carbon 63 (2013) 92–100.

[14] J. Xie, K.Z. Li, H.J. Li, Q.G. Fu, L.J. Guo, Effects of porous C/C density on the densification behavior and ablation property of C/C–ZrC–SiC composites, Carbon 57 (2013) 161–168.

[15] S.A. Chen, C.R. Zhang, Y.D. Zhang, D. Zhao, H.F. Hu, X. Xiong, Effects of polymer derived SiC interphase on the properties of C/ZrC composites, Mater. Des. 58 (2014) 102–107.

[16] S.F. Tang, J.Y. Deng, S.J. Wang, W.C. Liu, K. Yang, Ablation behaviors of ultra-high temperature ceramic composites, Mater. Sci. Eng., A 465 (2007) 1–7.

[17] A. Paul, S. Venugopal, J.G.P. Binner, B. Vaidhyanathan, A.C.J. Heaton, P.M. Brown, UHTC-carbon fibre composites: preparation, oxyacetylene torch testing and characterization, J. Eur. Ceram. Soc. 33 (2013) 423–432.

[18] C.L. Yan, R.J. Liu, Y.B. Cao, C.R. Zhang, D.K. Zhang, Ablation behavior and mechanism of C/ZrC, C/ZrC–SiC and C/SiC composites fabricated by polymer infiltration and pyrolysis process, Corros. Sci. 86 (2014) 131–141.

[19] Y. Zeng, X. Xiong, G.D. Li, Z.K. Chen, W. Sun, D.N. Wang, Microstruture and ablation behavior of carbon/carbon composites infiltrated with Zr–Ti, Carbon 54 (2013) 300–309.

[20] S.A. Chen, H.F. Hu, Y.D. Zhang, C.R. Zhang, Q.K. Wang, Effects of TaC amount on the properties of 2D C/SiC–TaC composites prepared via precursor infiltration and pyrolysis, Mater. Des. 51 (2013) 19–24.

[21] B. Feng, H.J. Li, Y.L. Zhang, L. Liu, M. Yan, Effect of SiC/ZrC ratio on the mechanical and ablation properties of C/C–SiC–ZrC composites, Corros. Sci. 82 (2014) 27–35.

[22] L. Liu, H.J. Li, X.H. Shi, W. Feng, Y.J. Wang, D.J. Yao, Effects of SiC addition on the ablation properties of C/C composites in different heat fluxes under oxyacetylene torch, Vacuum 90 (2013) 97–99.

[23] J. Yin, X. Xiong, H.B. Zhang, B.Y. Huang, Microstructure and ablation performances of dual-matrix carbon/carbon composites, Carbon 44 (2006) 1690–1694.

[24] S.A. Chen, C.R. Zhang, Y.D. Zhang, D. Zhan, H.F. Hu, Z.B. Zhang, Mechanism of ablation of 3D C/ZrC–SiC composite under an oxyacetylene flame, Corros. Sci. 68 (2013) 168–175.

[25] Z.Q. Li, H.J. Li, S.Y. Zhang, J. Wang, W. Li, F.J. Sun, Effect of reaction melt infiltration temperature on the ablation properties of 2D C/C–SiC–ZrC composites, Corros. Sci. 58 (2012) 12–19.

[26] L. Liu, H.J. Li, W. Feng, X.H. Shi, H. Wu, J.L. Zhu, Effect of surface ablation products on the ablation resistance of C/C–SiC composites under oxyacetylene torch, Corros. Sci. 67 (2013) 60–66.